

Guanylin and uroguanylin induce natriuresis in mice lacking guanylyl cyclase-C receptor

STEPHEN L. CARRITHERS, COBERN E. OTT, MICHAEL J. HILL, BRETT R. JOHNSON, WEIYAN CAI, JASON J. CHANG, RAJESH G. SHAH, CONGMEI SUN, ELIZABETH A. MANN, MANASSES C. FONTELES, LEONARD R. FORTE, BRIAN A. JACKSON, RALPH A. GIANNELLA, and RICHARD N. GREENBERG

Department of Internal Medicine, Division of Infectious Diseases, Lexington VA Medical Center and University of Kentucky, Lexington, Kentucky; Department of Physiology, University of Kentucky, Lexington, Kentucky; Department of Biological Chemistry & Molecular Pharmacology, Harvard Medical School, Harvard University, Boston, Massachusetts; Division of Digestive Diseases, University of Cincinnati and Cincinnati VA Medical Center, Cincinnati, Ohio; Clinical Research Unit of Federal University of Ceará and Ceará State University, Fortaleza, Brazil; Department of Pharmacology, Missouri University and Truman Memorial Veterans Hospital, Columbia, Missouri

Guanylin and uroguanylin induce natriuresis in mice lacking guanylyl cyclase-C receptor.

Background. Guanylin (GN) and uroguanylin (UGN) are intestinally derived peptide hormones that are similar in structure and activity to the diarrhea-causing *Escherichia coli* heat-stable enterotoxins (STa). These secretagogues have been shown to affect fluid, Na^+ , K^+ , and Cl^- transport in both the intestine and kidney, presumably by intracellular cyclic guanosine monophosphate (cGMP)-dependent signal transduction. However, the in vivo consequences of GN, UGN, and STa on renal function and their mechanism of action have yet to be rigorously tested.

Methods. We hypothesized that intravenous administration of GN, UGN, or STa would cause an increase in natriuresis in wild-type mice via cGMP and guanylyl cyclase-C (GC-C, *Gucy2c*), the only known receptor for these peptide-hormones, and that the peptide-induced natriuresis would be blunted in genetically altered mice devoid of GC-C receptors (GC-C^(-/-) null).

Results. In wild-type mice using a modified renal clearance model, GN, UGN, and STa elicited significant natriuresis, kaliuresis, and diuresis as well as increased urinary cGMP levels in a time- and dose-dependent fashion. Absolute and fractional urinary sodium excretion levels were greatest ~40 minutes following a bolus infusion with pharmacologic doses of these peptides. Unexpectedly, GC-C^(-/-) null mice also responded to the GN peptides similarly to that observed in wild-type mice. Glomerular filtration rate (GFR), blood pressure, and plasma cGMP in the mice (wild-type or GC-C^(-/-) null) did not significantly vary between the vehicle- and peptide-treatment groups. The effects of UGN may also influence long-term renal function due to down-regulation of the Na^+/K^+ ATPase γ -subunit and

the Cl^- channel CIC-K2 by 60% and 75%, respectively, as assessed by differential display polymerase chain reaction (PCR) (DD-PCR) and Northern blot analysis of kidney mRNA from mice treated with UGN.

Conclusion. GN, UGN, and STa act on the mouse kidney, in part, through a cGMP-dependent, GC-C-independent mechanism, causing significant natriuresis by renal tubular processes. UGN may have further long-term effects on the kidney by altering the expression of such transport-associated proteins as Na^+/K^+ ATPase and CIC-K2.

The kidney plays a critical role in the maintenance of extracellular fluid volume, and as a consequence, blood pressure, by regulating total body NaCl content [1, 2]. Fundamentally, alterations in NaCl content (either through changes in intake or through inappropriate extrarenal loss) lead to adjustments in urinary NaCl excretion that are designed to ultimately help restore normal levels. It is well established in both humans and in experimental animals that orally administered NaCl loads can be excreted more rapidly than equivalent salt loads administered intravenously [3–7]. These observations support a concept that NaCl intake may be monitored by the intestine, and that an increased delivery results in the generation of a signal to the kidney that begins to adjust sodium excretion to match intake *prior* to the absorption of sufficient NaCl to cause significant changes in extracellular fluid volume [8, 9]. For example, urinary sodium excretion is significantly elevated in the 4-hour period immediately after an oral salt load in rats, rabbits, and humans [3, 4, 6, 7, 10, 11]. In sharp contrast, an intravenous salt load of the same amount causes a much smaller increase in sodium excretion over the same time period. Thus, a putative “intestinal natriuretic factor” could link the intestine with the kidney as a means of regulating urinary salt excretion to match dietary salt intake.

Key words: kidney, cGMP, guanylyl cyclase, renal clearance, sodium, DD-PCR.

Received for publication January 21, 2003
and in revised form April 4, 2003, and July 7, 2003
Accepted for publication August 18, 2003

Studies from this and other laboratories suggest that two low-molecular-weight peptides, guanylin (GN) and uroguanylin (UGN), may be critical components of this enterorenal axis [9, 12–14]. In the gastrointestinal tract, GN and UGN bind to and activate guanylyl cyclase-C (GC-C) [15], an apical membrane receptor that has an intrinsic guanylyl cyclase catalytic domain [16]. Mechanistically, receptor activation enhances intracellular guanosine-3',5'-cyclic monophosphate (cGMP) synthesis, which in turn, stimulates intestinal electrogenic chloride and bicarbonate secretion via the cystic fibrosis transmembrane conductance regulator (CFTR) chloride channel and inhibits electroneutral sodium absorption [9, 15, 17]. Although GN was initially isolated from jejunum and UGN from urine, these peptides have been found throughout the intestine where they are released from specific epithelial cells into both the lumen and the systemic circulation [9, 18–21]. GN and UGN are structurally similar to the heat-stable enterotoxin (STa) peptides secreted by pathogenic strains of enteric bacteria [9, 22]. These toxins virtually act as superagonists of GC-C and trigger nonphysiologic movement of electrolytes within the intestinal lumen [23].

Recent studies from this laboratory have shown that GN and UGN can also affect renal function. Intravenous administration of exogenous GN and UGN induce significant natriuresis in mice [12, 24]. In addition, studies in the isolated perfused rat kidney have shown that both peptides are natriuretic in a time- and dose-dependent fashion [14, 25]. Coincident with these solute excretory patterns, urinary cGMP excretion also increased after peptide administration. GN, UGN, and STa have also been shown to elevate cGMP in organ-cultured kidney slices and proximal convoluted tubule cells in vitro [26–29]. Consistent with these functional responses, previous studies have reported ^{125}I -GN [30] and ^{125}I -ST binding [27, 31], and GC-C mRNA expression in heterogeneous kidney preparations [32–34]. Employing semi-quantitative reverse transcription-polymerase chain reaction (RT-PCR), we assessed the distribution of renal GN/UGN receptor mRNA in specific microdissected segments of the rat nephron [32]. These results suggest that GN/UGN/STa may affect transport in multiple nephron segments that are involved in renal tubular handling of NaCl since receptor mRNA expression is relatively high in the collecting tubules, the proximal convoluted tubule, and the medullary thick ascending limb. Lower levels of receptor mRNA were observed in the cortical thick ascending limb, distal convoluted tubules, and glomeruli.

While the mechanisms that regulate the renal effects of GN and UGN are unclear, a role for sodium intake has been implicated. For example, the UGN concentration in human urine and plasma is increased during a high salt intake [34]. Additionally, perfusion of the small intestine [35] and colon [36] in situ with hypertonic NaCl solutions

markedly increased GN (and to a lesser degree UGN) secretion into the lumen, while perfusion with similar osmotic concentrations of mannitol exhibited much lower effects [21, 37]. However, in a whole animal model of osmotic diarrhea (using a lactose-based diet), GN and UGN mRNA and protein expression levels were significantly increased suggesting that these genes are responsive to the increased intraluminal hypertonicity inherent to the model [21]. Furthermore, using HT29-18-N2 colonic cells, hypertonic solutions (of NaCl, lactose, or mannitol) were found to significantly increase GN and UGN expression and secretion from the apical and basolateral surfaces of the cell [18]. Conversely, low NaCl intake down-regulates GN mRNA and peptide expression in the distal colon [38]. Recent studies from this laboratory have further examined the effects of altered NaCl intake on GN and UGN mRNA expression in the four principal regions of the rat intestine—duodenum, jejunum, ileum, and the colon—and have shown that both peptides are affected by salt diet in the rat intestine [39]. More important, expression patterns could be affected within 4 hours of an intragastric administration of NaCl, suggesting that a putative signaling system can respond rapidly to altered NaCl intake.

Although these data are compelling and support a hypothesis that the renal effects of intestinally derived GN and UGN are involved in the maintenance of salt and water homeostasis, no detailed analysis of the renal action and mechanism of natriuresis by these peptides have been rigorously evaluated. Therefore, the principal aim of the present study was to elucidate the renal effects and the mechanism(s) of GN and UGN action in vivo employing a modified mouse clearance model. In addition, to address the renal mechanism by which these peptides elicit natriuresis, we evaluated how this system acts in GC-C^(-/-) null (*Gucy2c* ^{-/-}) mice. Here, we show that intravenous administration of GN and UGN increase absolute and fractional sodium excretion in wild-type and GC-C^(-/-) null mice in a rapid, time- and dose-dependent fashion. It has been assumed that the renal effects of GN/UGN are mediated by peptide binding to GC-C [9, 32, 40]. However, data in this report would suggest the presence of an alternate renal GN/UGN/STa receptor. Therefore, a second goal of the present study was to begin to address, using a molecular approach, the presence of this GC-C independent mechanism of renal GN/UGN action.

EXPERIMENTAL PROCEDURES

Mouse models

Mice lacking the GC-C receptor were generated as previously described [41]. Embryonic stem cells (E14TG2A from strain 129/Sv), selected for a targeted deletion of Exon 1 of *Gucy2c*, the gene encoding GC-C, were microinjected into Black Swiss blastocysts. Germline

chimeric offspring were identified and bred with Black Swiss mice. The resulting heterozygous littermates (hybrids of 129/Sv and Black Swiss) were bred to produce homozygous *Gucy2c*^{-/-} (GC-C^(-/-) null) and *Gucy2c*^{+/+} (wild-type) mice. The GC-C^(-/-) null and wild-type mice used in these experiments are the progeny of these F2 mice. In addition, NIH Institute of Cancer Research/Harlan Sprague-Dawley (ICR-HSD) mice were also used as wild-type controls.

Suckling mouse intestinal fluid assay

In order to assess the potency and bioactivity of GN, UGN, and STa, the peptides were tested for their ability to induce intestinal fluid accumulation in newborn mice, as described previously [12, 42]. ICR-HSD suckling mice, 2 to 4 days old (2.1 ± 1.0 g), were dosed orally with 0.1 mL of test solution. The injections contained vehicle (1 mmol/L HEPES and 0.1% Evans blue dye) alone or the peptides dissolved in vehicle (except that GN injections contained the protease inhibitors chymostatin (0.1 mmol) and aprotinin (0.67 U) [24, 25]). After administration of vehicle or peptide agonists, the mice were kept at room temperature for 3 hours. The mice were then killed, intestinal and body weights measured, and a ratio of the intestinal weight to remaining body weight was calculated. A ratio of 0.0875 represents one mouse unit of activity, indicating significant fluid accumulation in the intestine. The secretion activity (one unit) of GN (containing aprotinin and chymostatin) was 142.9 ± 5.3 ng/mouse; UGN was 41.5 ± 1.7 ng/mouse; and for STa, 3.75 ± 0.2 ng/mouse.

Stability of GN, UGN, and STa in mouse serum

Approximately 4 units of peptide activity (GN, 550 ng; UGN, 150 ng; STa, 15 ng) were incubated in 100 μ L of mouse serum for 120 minutes at 37°C under 5% CO₂. Samples were mixed with an equal volume of vehicle (1 mmol/L HEPES and 0.1% Evans blue dye) and administered to suckling mice. The fluid accumulation in the intestine was assessed for each peptide-containing sample containing the mouse serum or vehicle alone (control). The mean \pm SEM from four to five mice/group was used in determining representative fluid accumulation and compared against that of the control group (peptide-induced group without serum). Mouse plasma alone did not significantly increase the fluid volume in the suckling mouse intestine.

In vitro cGMP accumulation assay

The bioactivity of each peptide cGMP agonist (GN, UGN, and STa) was tested in an in vitro tissue culture-based cGMP accumulation assay as previously described using T84 cells [43–45]. Briefly, T84 cells, grown as monolayers in 24-well plates, were washed twice with 1 mL serum-free Dulbecco's modified Eagle's

medium (DMEM)-F12 media (Gibco-Life Technologies, Gaithersburg, MD, USA). The sample (0.2 mL) was layered onto the cells and incubated for 40 minutes at 37°C. The media were removed, and the cells were washed twice with serum-free media. Cells were lysed and peptide-induced cGMP was measured using a specific nonradioactive enzyme-linked immunosorbent assay (ELISA) (Amersham-Pharmacia, Piscataway, NJ, USA), and protein was measured (Bio-Rad, Hercules, CA, USA) using bovine serum albumin (BSA) as standard. The bioactivity, which is represented as pmol cGMP produced/min/mL, was a direct measure of the amount of GC-C stimulating peptide present in a particular sample. Sensitivity for this bioassay approaches 1 pmol cGMP/well/mg protein, which is similar to the sensitivity found previously [43, 44].

Mouse clearance-renal function assay

Six-week old male ICR/HSD mice (Harlan) (colony bred), weighing 21.5 ± 0.7 g, were used in a modified mouse clearance model where the bladder was catheterized and/or the urethra sealed prior to vehicle or peptide administration [12, 24]. Each mouse was exposed to methoxyflurane in a desiccator or 5% halothane in O₂ using a mouse ventilation system until the mouse was unconscious (approximately 1 to 3 minutes). At this time, the abdominal region was shaved and a 25-gauge needle was inserted through the skin to the visible bladder. Urine was aspirated (and saved) and the bladder emptied. The urethra was then cannulated by polyethylene (PE-10) tubing and/or sealed shut with surgical glue (Vet Bond (methyl 2-cyanoacrylate) (Midwest Veterinary Supply; Madison, WI, USA) and the mouse was placed in a restrainer to limit excessive movement. Fifty microliters of test solution [0.1% Evans blue dye in isotonic saline (vehicle) with or without peptide agonist] was injected into the tail vein. A subset of mice, which did not receive a tail vein injection, was also included for timed controls. After the indicated time (0 to 120 minutes), the animal was again exposed to methoxyflurane, the bladder contents emptied, and the urine volume recorded. A mouse was used for each time point (e.g., 20, 40, 60, 80, and 120 minutes) ($N = 6$ –8 mice per time point). The mouse was sacrificed by open chest pneumothorax at which point a blood sample was drawn and the kidneys were removed for nephron segment isolation and/or renal zone RNA isolation. The distal colon was also removed for RNA isolation. In a separate set of experiments, the blood pressure and heart rate were also measured. Urine and plasma sodium, potassium, cGMP, cyclic adenosine monophosphate (cAMP), creatinine, and osmolality were measured. Sodium and potassium were determined by flame photometry (Instrumentation Laboratory Autocal Flame Photometer Model 643,

Lexington, MA, USA) and osmolality was measured by an osmometer (Wescor 5100B Vapor Pressure Osmometer, Logan, UT, USA). cGMP and cAMP were measured by nonradioactive ELISA (Amersham-Pharmacia). Urinary and plasma creatinine was measured by a spectrophotometric assay (Sigma Chemical Co., St. Louis, MO, USA). Glomerular filtration rate (GFR) was determined as creatinine clearance. The mice were not allowed to eat 24 hours prior to the experiment, although they were allowed to drink ad libitum. Their diet had consisted of 18% crude protein, 9% crude fat, 4% crude fiber, and 11% crude moisture containing 0.6% NaCl (final net Na⁺ concentration of 0.2%) (Prolab Rat, Mouse, Hamster 2000).

Messenger RNA differential display PCR

Differential display was performed on 100 ng of normalized DNase-treated whole kidney RNA as described previously [12]. Specific amplified products that showed a difference in the display pattern between the UGN-treated and timed vehicle-treated control mice were selected for subcloning. Luminescent paint dots were used to align the autoradiogram and gel, and only the single most intense center band of a multiple band series was excised from the dried gel. This excised band with attached Whatman paper was rehydrated in 100 μ L of water and eluted at room temperature for 10 minutes followed by 100°C for 15 minutes. After cooling, the paper and gel pieces were removed and DNA was precipitated, washed in ethanol, and resuspended in H₂O. The band was amplified by PCR again, and an aliquot was analyzed on a 1.5% agarose gel to confirm amplification of the cDNA band of interest. The product was ligated into the pSTBlue-1 multipurpose cloning vector for sequencing, which was performed by the University of Kentucky Sequencing Core Facility.

RNA extraction and Northern blot analysis

Total RNA was extracted from whole kidney, renal cortex, and colon with Trizol. The concentration and purity of the isolated RNA was assessed by ultraviolet spectrophotometry. For generation of the molecular probe, total RNA (0.1 μ g) from the renal cortex from GC-C^(-/-) null mice was treated with RNase-free DNase to remove genomic DNA, and was subjected to reverse transcription(RT)-PCR using thermal cycling conditions and primers as described previously [32]. Primers for PCR directed against mouse intestinal/renal GC-C were selected to cross an intron-exon junction [32, 40, 41]. The target band of expected size (~400 bp) was gel-isolated, followed by subcloning into the pSTBlue-1 multipurpose cloning vector (Novagen, EMD Biosciences, San Diego, CA, USA). Sequencing was performed by the University of Kentucky Sequencing Core Facility. The 400 bp

product obtained from the GC-C^(-/-) null mouse kidney cortex was 89% similar to the extracellular region of mouse intestinal GC-C.

Approximately 25 μ g of total RNA extracted from colonic cells lining the intestinal lumen and kidney cortex was run on a denaturing 1.2% agarose formaldehyde gel (2.2 mol/L formaldehyde) and transferred to a positively-charged nylon membrane (ICN, Costa Mesa, CA, USA) for Northern analysis. Labeled probes (which include murine cDNA fragments from the extracellular domain of GC-C [40, 41], Na⁺/K⁺-ATPase γ -subunit [46], and ClC-K2 chloride channel[47]) were used during hybridization employing ExpressHyb solution (Clontech, Palo Alto, CA, USA) following manufacturers' protocol. Membranes were washed two times with 2 \times standard sodium citrate (SSC)/1% sodium dodecyl sulfate (SDS) solution (SSC = 150 mmol/L NaCl, 15 mmol/L sodium citrate, pH 7.0) at 68°C followed by two washes with 0.1 \times SSC/0.05% SDS at 68°C. One final membrane wash of 2 \times SSC was performed at room temperature prior to autoradiography and phosphoimaging. Equal loading of RNA was shown by subsequent hybridization with β -actin. For visual purposes, blots were developed following 3, 7, and 14 days exposure to film.

Statistical analysis

Results are presented as the mean \pm standard error of the mean (SEM). The number (*N*) for each experiment indicates the number of animals used in each experiment or data point. Using the Student paired *t* test, we assessed the statistical significance of the data with each effect compared to its own timed control. Specific differences between groups and time points were also determined by one-way analysis of variance (ANOVA) for unpaired groups with post hoc Newman-Keuls multiple range test or paired ANOVA with post hoc Tukey test. Significance was taken as *P* < 0.05.

RESULTS

In vitro stability studies of GN, UGN, and STa

Peptide stability studies were performed prior to performing clearance experiments to determine the stability of GN, UGN, and STa in mouse serum. Previously, we have shown in both the suckling mouse and the isolated perfused rat kidney that the three-dimensional structure and multiple disulfide bonds of UGN and STa provide protection from enzymatic degradation under both in vivo and in vitro conditions [14, 24, 25, 48]. However, GN possesses a chymotrypsin-sensitive bond within its primary 15 amino acid structure [9]. Studies with chymotrypsin inhibitors with GN confer protection and increase the activity of this peptide in vivo [24, 25]. Therefore, the present study tested and compared the stability

Table 1. Guanylin-induced changes in renal function in mice

	Dose $\mu\text{g/kg}$ <i>body weight</i>	Time <i>minutes</i>				
Guanylin		20	40	60	80	120
Urinary flow $\mu\text{L/min}$						
Vehicle ^{a,b}	0.00	2.93 \pm 0.29	2.31 \pm 0.20	1.73 \pm 0.29	1.62 \pm 0.14	1.41 \pm 0.23
1 unit	6.8 \pm 0.1	4.05 \pm 0.63	4.35 \pm 0.75 ^c	1.98 \pm 0.34	1.64 \pm 0.21	1.47 \pm 0.12
3 units	19.6 \pm 0.2	4.96 \pm 0.65 ^c	5.01 \pm 0.10 ^c	2.78 \pm 0.33 ^c	2.18 \pm 0.12	2.08 \pm 0.26
10 units	64.4 \pm 0.6	6.40 \pm 0.89 ^c	6.60 \pm 0.61 ^c	4.47 \pm 0.55 ^c	3.41 \pm 0.32 ^c	2.42 \pm 0.33 ^c
30 units	195.4 \pm 2.7	4.55 \pm 1.00 ^c	4.28 \pm 0.35 ^c	3.94 \pm 0.25 ^c	3.05 \pm 0.74 ^c	2.35 \pm 0.11 ^c
Glomerular filtration rate $\mu\text{L/min}$						
Vehicle	0.00	175.6 \pm 65.4	170.7 \pm 79.5	164.1 \pm 36.3	156.9 \pm 46.7	141.1 \pm 62.1
1 unit	6.8 \pm 0.1	185.4 \pm 45.5	172.3 \pm 63.9	160.5 \pm 59.4	155.4 \pm 41.0	149.1 \pm 55.5
3 units	19.6 \pm 0.2	176.9 \pm 42.0	165.2 \pm 45.9	155.4 \pm 49.5	145.8 \pm 39.4	138.6 \pm 48.7
10 units	64.4 \pm 0.6	170.5 \pm 51.7	155.8 \pm 53.6	142.8 \pm 43.8	132.5 \pm 29.7	120.6 \pm 37.8
30 units	195.4 \pm 2.7	161.4 \pm 55.3	149.1 \pm 39.7	136.1 \pm 56.1	125.1 \pm 33.3	121.5 \pm 30.4
$\text{U}_{\text{Na}}\text{V}$ $\mu\text{Eq/min}$						
Vehicle	0.00	0.475 \pm 0.121	0.403 \pm 0.073	0.354 \pm 0.065	0.319 \pm 0.136	0.254 \pm 0.119
1 unit	6.8 \pm 0.1	0.675 \pm 0.141	0.710 \pm 0.107	0.570 \pm 0.104	0.385 \pm 0.078	0.263 \pm 0.046
3 units	19.6 \pm 0.2	1.017 \pm 0.118 ^c	0.812 \pm 0.100 ^c	0.610 \pm 0.064 ^c	0.446 \pm 0.034	0.366 \pm 0.080
10 units	64.4 \pm 0.6	1.397 \pm 0.117 ^c	1.035 \pm 0.094 ^c	0.880 \pm 0.087 ^c	0.595 \pm 0.029 ^c	0.363 \pm 0.040
30 units	195.4 \pm 2.7	1.113 \pm 0.171 ^c	0.951 \pm 0.106 ^c	0.900 \pm 0.077 ^c	0.719 \pm 0.113 ^c	0.457 \pm 0.035 ^c
$\text{U}_{\text{K}}\text{V}$ $\mu\text{Eq/min}$						
Vehicle	0.00	0.268 \pm 0.073	0.249 \pm 0.020	0.238 \pm 0.034	0.212 \pm 0.027	0.172 \pm 0.029
1 unit	6.8 \pm 0.1	0.368 \pm 0.155	0.303 \pm 0.066	0.298 \pm 0.024	0.254 \pm 0.043	0.176 \pm 0.018
3 units	19.6 \pm 0.2	0.500 \pm 0.094 ^c	0.458 \pm 0.049 ^c	0.468 \pm 0.089 ^c	0.293 \pm 0.082 ^c	0.209 \pm 0.044
10 units	64.4 \pm 0.6	0.609 \pm 0.133 ^c	0.564 \pm 0.112 ^c	0.705 \pm 0.200 ^c	0.473 \pm 0.141 ^c	0.245 \pm 0.022 ^c
30 units	195.4 \pm 2.7	0.731 \pm 0.162 ^c	0.725 \pm 0.134 ^c	0.690 \pm 0.125 ^c	0.524 \pm 0.118 ^c	0.288 \pm 0.031 ^c
Osmolality mOsm/kg						
Vehicle	0.00	963.8 \pm 128.3	991.1 \pm 61.2	1012.6 \pm 74.2	1081.7 \pm 54.4	1093.8 \pm 72.7
1 unit	6.8 \pm 0.1	1237.0 \pm 98.5	972.5 \pm 85.5	1070.3 \pm 134.7	1072.0 \pm 95.5	871.0 \pm 119.9
3 units	19.6 \pm 0.2	836.8 \pm 73.8	976.5 \pm 60.2	1178.4 \pm 113.3	1076.0 \pm 80.2	933.8 \pm 32.7
10 units	64.4 \pm 0.6	919.1 \pm 69.4	1184.3 \pm 85.6	1188.3 \pm 260.0	1084.2 \pm 115.6	1155.9 \pm 127.3
30 units	195.4 \pm 2.7	1311.4 \pm 152.6	1280.9 \pm 116.9	945.2 \pm 160.6	1320.3 \pm 126.5	1353.8 \pm 153.6

Abbreviations are: $\text{U}_{\text{Na}}\text{V}$, sodium excretion; $\text{U}_{\text{K}}\text{V}$, potassium excretion.

^aTimed vehicle-controls represent the value obtained from mice treated (intravenous bolus) simultaneously with an equal volume of vehicle without peptide. Baseline controls (preinjected control values) were obtained from a 30 μL aliquot of blood and the urine (from the bladder) 30 minutes prior to the intravenous administration of vehicle or peptide. Plasma and urinary sodium, potassium, osmolality, and creatinine were obtained prior to and after each time point from the timed vehicle-control and peptide-treated mice. Baseline controls were: urinary flow, 1.89 \pm 0.16 $\mu\text{L/min}$; glomerular filtration rate, 188.1 \pm 50.3 $\mu\text{L/min}$; $\text{U}_{\text{Na}}\text{V}$, 0.694 \pm 0.099 $\mu\text{Eq/min}$; $\text{U}_{\text{K}}\text{V}$, 0.223 \pm 0.043 $\mu\text{Eq/min}$; osmolality, 950.1 \pm 60.3 mOsm/kg .

^bValues are means \pm standard error of the mean ($N = 6-8$ mice/group).

^c $P \leq 0.05$ compared to the respective timed-vehicle control group.

of GN (in the presence of chymotrypsin inhibitors), UGN, and STa in mouse serum. Known amounts of each bioactive peptide (which were previously assessed by the suckling mouse assay) were added to 100 μL of mouse serum in a culture tube and incubated at 37°C at pH 7.4 under 5% CO_2 atmosphere for 120 minutes. Following incubation, 50 μL of the test samples were combined with an equal volume of vehicle and administered to suckling mice. GN, UGN, and STa all retained >95% activity over 2 hours in mouse serum.

Intravenous administration of GN, UGN, and STa in mice

To address the question whether GN and UGN significantly affect renal function in vivo, experiments were designed to measure the urine output, sodium and potassium excretion, urinary cyclic nucleotide levels, and urine osmolality after intravenous injections of the agonist-peptides. Employing the modified mouse renal clearance assay developed in this laboratory [12, 24], we demonstrated that both GN and UGN cause an increase in urine volume and total urinary sodium and potassium excretion

in a time- and dose-dependent fashion when compared to timed-vehicle control-injected mice (Tables 1 and 2). The urine osmolalities did not significantly vary between the control and treated groups nor were they significantly altered with respect to the time of assay (0 to 120 minutes) or dose of peptide (0 to 30 units). The most profound increase in absolute urinary sodium and potassium excretion was observed within 40 minutes after intravenous peptide injection, regardless of the dose of GN or UGN administered to the mice. The level of natriuresis by GN and UGN appear to decrease gradually after 40 minutes following peptide injection. For example, 40 minutes postinjection of 30 units of GN in mice increased the sodium excretion ($\text{U}_{\text{Na}}\text{V}$) by 2.36-fold over the timed-vehicle controls (0.403 \pm 0.073 to 0.951 \pm 0.106 $\mu\text{Eq/min}$) and UGN (30 units, 40-min post-injection) increased sodium excretion by 4.20-fold (0.403 \pm 0.073 to 1.694 \pm 0.231 $\mu\text{Eq/min}$). After 120 min, GN (30 units) increased the sodium excretion by only 1.80-fold over the timed-vehicle controls (0.254 \pm 0.119 $\mu\text{Eq/min}$ to 0.457 \pm 0.035 $\mu\text{Eq/min}$) and UGN (30 units, 120 minutes postinjection)

Table 2. Uroguanylin-induced changes in renal function in mice

		Time <i>minutes</i>				
Uroguanylin	Dose $\mu\text{g/kg}$ <i>body weight</i>	20	40	60	80	120
Urinary flow $\mu\text{L/min}$						
Vehicle ^{a,b}	0.00	2.93 \pm 0.29	2.31 \pm 0.20	1.73 \pm 0.29	1.62 \pm 0.14	1.41 \pm 0.23
1 unit	1.9 \pm 0.1	3.35 \pm 0.35	3.45 \pm 0.30	2.71 \pm 0.37	2.43 \pm 0.25	2.03 \pm 0.32
3 units	5.6 \pm 0.1	3.71 \pm 0.64	3.81 \pm 0.35	3.02 \pm 0.31 ^c	2.63 \pm 0.15 ^c	2.57 \pm 0.38 ^c
10 units	18.8 \pm 0.3	5.50 \pm 0.33 ^c	5.80 \pm 0.95 ^c	3.58 \pm 0.35 ^c	3.09 \pm 0.11 ^c	2.98 \pm 0.20 ^c
30 units	56.3 \pm 0.7	8.69 \pm 1.21 ^c	8.80 \pm 0.97 ^c	4.81 \pm 0.33 ^c	4.33 \pm 0.73 ^c	2.90 \pm 0.27 ^c
Glomerular filtration rate $\mu\text{L/min}$						
Vehicle	0.00	175.6 \pm 65.4	170.7 \pm 79.5	164.1 \pm 36.3	156.9 \pm 46.7	141.1 \pm 62.1
1 unit	1.9 \pm 0.1	181.2 \pm 33.9	172.5 \pm 59.7	170.2 \pm 47.9	149.8 \pm 20.1	140.5 \pm 23.3
3 units	5.6 \pm 0.1	170.5 \pm 30.0	164.8 \pm 42.6	150.1 \pm 28.4	135.2 \pm 24.6	131.7 \pm 42.0
10 units	18.8 \pm 0.3	169.3 \pm 26.3	158.5 \pm 31.4	135.4 \pm 27.9	125.5 \pm 28.5	110.1 \pm 19.8
30 units	56.3 \pm 0.7	159.1 \pm 30.1	147.8 \pm 25.3	122.4 \pm 20.7	120.7 \pm 22.2	109.8 \pm 16.7
$\text{U}_{\text{Na}}\text{V}$ $\mu\text{Eq/min}$						
Vehicle	0.00	0.475 \pm 0.121	0.403 \pm 0.073	0.354 \pm 0.065	0.319 \pm 0.136	0.254 \pm 0.119
1 unit	1.9 \pm 0.1	1.176 \pm 0.127 ^c	0.809 \pm 0.091 ^c	0.640 \pm 0.103 ^c	0.482 \pm 0.044	0.287 \pm 0.039
3 units	5.6 \pm 0.1	1.308 \pm 0.145 ^c	0.959 \pm 0.078 ^c	0.779 \pm 0.069 ^c	0.611 \pm 0.085 ^c	0.490 \pm 0.042 ^c
10 units	18.8 \pm 0.3	1.684 \pm 0.248 ^c	1.421 \pm 0.116 ^c	1.112 \pm 0.109 ^c	0.841 \pm 0.056 ^c	0.637 \pm 0.039 ^c
30 units	56.3 \pm 0.7	2.097 \pm 0.359 ^c	1.694 \pm 0.231 ^c	1.491 \pm 0.070 ^c	0.859 \pm 0.128 ^c	0.587 \pm 0.079 ^c
$\text{U}_{\text{K}}\text{V}$ $\mu\text{Eq/min}$						
Vehicle	0.00	0.268 \pm 0.073	0.249 \pm 0.020	0.238 \pm 0.034	0.212 \pm 0.027	0.172 \pm 0.029
1 unit	1.9 \pm 0.1	0.505 \pm 0.063 ^c	0.421 \pm 0.039	0.322 \pm 0.046	0.224 \pm 0.033	0.233 \pm 0.038
3 units	5.6 \pm 0.1	0.597 \pm 0.104 ^c	0.598 \pm 0.081 ^c	0.425 \pm 0.075 ^c	0.258 \pm 0.040	0.253 \pm 0.039
10 units	18.8 \pm 0.3	0.683 \pm 0.116 ^c	0.610 \pm 0.096 ^c	0.390 \pm 0.025 ^c	0.324 \pm 0.051 ^c	0.289 \pm 0.023 ^c
30 units	56.3 \pm 0.7	0.718 \pm 0.097 ^c	0.617 \pm 0.067 ^c	0.394 \pm 0.049 ^c	0.297 \pm 0.041 ^c	0.238 \pm 0.007 ^c
Osmolality <i>mOsm/kg</i>						
Vehicle	0.00	963.8 \pm 128.3	991.1 \pm 61.2	1012.6 \pm 74.2	1081.7 \pm 54.4	1093.8 \pm 72.7
1 unit	1.9 \pm 0.1	1060.5 \pm 115.0	935.4 \pm 58.6	879.5 \pm 30.4	869.8 \pm 154.7	916.5 \pm 123.6
3 units	5.6 \pm 0.1	1222.3 \pm 191.8	1014.1 \pm 76.9	1056.3 \pm 154.2	1002.8 \pm 184.3	822.2 \pm 73.3
10 units	18.8 \pm 0.3	1249.7 \pm 199.5	1052.3 \pm 55.5	1204.7 \pm 129.0	1212.6 \pm 127.4	902.2 \pm 56.1
30 units	56.3 \pm 0.7	886.4 \pm 44.0	934.6 \pm 52.2	1022.2 \pm 159.7	876.7 \pm 71.6	1093.2 \pm 82.0

Abbreviation are: $\text{U}_{\text{Na}}\text{V}$, sodium excretion; $\text{U}_{\text{K}}\text{V}$, potassium excretion.

^aTimed vehicle- and baseline- (preinjected) control values were determined as described in Table 1. Plasma and urinary sodium, potassium, osmolality, and creatinine were obtained prior to and after each time point (0, 20, 40, 60, 80, and 120 minutes) from the timed vehicle-control and peptide-treated groups. Baseline (preinjected) controls were: urinary flow, 1.89 \pm 0.16 $\mu\text{L/min}$; glomerular filtration rate, 188.1 \pm 50.3 $\mu\text{L/min}$; $\text{U}_{\text{Na}}\text{V}$, 0.694 \pm 0.099 $\mu\text{Eq/min}$; $\text{U}_{\text{K}}\text{V}$, 0.223 \pm 0.043 $\mu\text{Eq/min}$; osmolality, 950.1 \pm 60.3 mOsm/kg .

^bValues are means \pm standard error of the mean ($N = 6-8$ mice/group).

^c $P \leq 0.05$ compared to the respective timed-vehicle control group.

increased by only 2.31-fold (0.254 \pm 0.119 $\mu\text{Eq/min}$ to 0.587 \pm 0.079 $\mu\text{Eq/min}$). Thus, the natriuretic effects of GN and UGN are transient in vivo.

UGN induced greater sodium excretion than GN at each time point of the assay. However, increased rate of potassium excretion ($\text{U}_{\text{K}}\text{V}$) was similar for both peptides. As shown in Table 3, STa elicited a greater natriuresis than GN or UGN; potassium excretion by STa was similar to that of GN and UGN. Although sodium and potassium excretion increased following GN, UGN, and STa administration, GFR decreased in a time-dependent fashion ($P > 0.05$). This trend suggests the contribution of a tubular, rather than a hemodynamic, mechanism for sodium excretion by the peptides. Plasma levels of the cyclic nucleotides cGMP and cAMP were also not significantly affected by peptide administration.

Exogenous intravenous administration of GN, UGN, or STa in mice significantly increased fractional sodium excretion (FE_{Na}) and urinary cGMP (FE_{cGMP}) (Fig. 1). Fractional excretion of sodium and potassium by GN, UGN, and STa significantly increased as a function of time compared to the timed-vehicle control mice. Maxi-

mal fractional sodium excretion was observed at approximately 40 minutes postinjection while fractional sodium excretion decreased toward the endpoint of the assay (120 minutes). Elevated urinary cGMP levels are coincident with the increased peptide-induced sodium excretion (Fig. 1, inset). Indeed, all three peptides caused an elevation of fractional cGMP excretion compared to control mice.

Neither blood pressure nor heart rate were affected by intravenous peptide administration in the mice. For example, the mean blood pressure in control mice (preinjection vs. vehicle-treated) after 60 minutes was 84.9 \pm 10.8 mm Hg and 87.5 \pm 12.8 mm Hg ($N = 3$), respectively, and the heart rate slightly increased from 353 \pm 15 bpm to 408 \pm 42 bpm ($N = 3$, $P > 0.05$). With a 10 unit (18.8 $\mu\text{g/kg}$ body weight) UGN bolus injection, the mean blood pressure after 60 minutes was (preinjection vs. peptide-treated) 85.1 \pm 3.3 mm Hg and 90.7 \pm 3.2 mm Hg ($N = 4$), respectively, and the heart rate increased from 418 \pm 19 bpm to 465 \pm 20 bpm ($N = 4$, $P > 0.05$). Intravenous administration of GN and STa also showed no significant changes in heart rate or mean blood pressure.

Table 3. Heat-stable enterotoxins (STa)-induced changes in renal function in mice

STa	Dose $\mu\text{g/kg}$ <i>body weight</i>	Time <i>minutes</i>				
		20	40	60	80	120
Urinary flow $\mu\text{L/min}$						
Vehicle ^{a,b}	0.00	2.93 \pm 0.29	2.31 \pm 0.20	1.73 \pm 0.29	1.62 \pm 0.14	1.41 \pm 0.23
1 unit	0.18 \pm 0.01	3.13 \pm 0.24	3.20 \pm 0.26 ^c	2.58 \pm 0.08 ^c	2.42 \pm 0.11 ^c	1.61 \pm 0.21
3 units	0.54 \pm 0.01	5.25 \pm 0.60 ^c	5.31 \pm 0.38 ^c	3.45 \pm 0.47 ^c	3.35 \pm 0.17 ^c	1.87 \pm 0.14
10 units	1.72 \pm 0.03	6.45 \pm 0.45 ^c	6.62 \pm 0.58 ^c	3.82 \pm 0.60 ^c	3.86 \pm 0.31 ^c	2.01 \pm 0.19
30 units	5.24 \pm 0.08	7.50 \pm 0.81 ^c	7.60 \pm 0.77 ^c	3.98 \pm 0.55 ^c	3.62 \pm 0.28 ^c	2.11 \pm 0.22 ^c
Glomerular filtration rate $\mu\text{L/min}$						
Vehicle	0.00	175.6 \pm 65.4	170.7 \pm 79.5	164.1 \pm 36.3	156.9 \pm 46.7	141.1 \pm 62.1
1 unit	0.18 \pm 0.01	176.2 \pm 52.8	169.4 \pm 71.3	165.2 \pm 69.1	149.5 \pm 54.8	138.5 \pm 51.8
3 units	0.54 \pm 0.01	177.8 \pm 61.0	158.7 \pm 55.7	139.8 \pm 48.3	133.1 \pm 35.6	132.4 \pm 57.2
10 units	1.72 \pm 0.03	164.3 \pm 48.2	147.4 \pm 54.9	129.5 \pm 42.9	125.5 \pm 29.7	121.8 \pm 30.1
30 units	5.24 \pm 0.08	161.2 \pm 40.7	139.9 \pm 33.5	121.3 \pm 36.6	111.5 \pm 21.4	110.8 \pm 28.4
$\text{U}_{\text{Na}}\text{V}$ $\mu\text{Eq/min}$						
Vehicle	0.00	0.475 \pm 0.121	0.403 \pm 0.073	0.354 \pm 0.065	0.319 \pm 0.136	0.254 \pm 0.119
1 unit	0.18 \pm 0.01	0.620 \pm 0.080	0.540 \pm 0.036	0.481 \pm 0.042	0.419 \pm 0.032	0.292 \pm 0.025
3 units	0.54 \pm 0.01	1.135 \pm 0.260 ^c	1.002 \pm 0.128 ^c	0.890 \pm 0.116 ^c	0.773 \pm 0.065 ^c	0.382 \pm 0.049
10 units	1.72 \pm 0.03	1.402 \pm 0.333 ^c	1.212 \pm 0.140 ^c	1.059 \pm 0.289 ^c	0.885 \pm 0.101 ^c	0.489 \pm 0.093
30 units	5.24 \pm 0.08	1.734 \pm 0.409 ^c	1.510 \pm 0.410 ^c	1.349 \pm 0.145 ^c	1.010 \pm 0.042 ^c	0.553 \pm 0.087 ^c
$\text{U}_{\text{K}}\text{V}$ $\mu\text{Eq/min}$						
Vehicle	0.00	0.268 \pm 0.073	0.249 \pm 0.020	0.238 \pm 0.034	0.212 \pm 0.027	0.172 \pm 0.029
1 unit	0.18 \pm 0.01	0.392 \pm 0.068	0.351 \pm 0.036	0.299 \pm 0.035	0.288 \pm 0.055	0.182 \pm 0.027
3 units	0.54 \pm 0.01	0.456 \pm 0.057 ^c	0.401 \pm 0.049 ^c	0.341 \pm 0.121	0.310 \pm 0.058	0.208 \pm 0.040
10 units	1.72 \pm 0.03	0.616 \pm 0.161 ^c	0.511 \pm 0.075 ^c	0.397 \pm 0.061 ^c	0.312 \pm 0.072 ^c	0.232 \pm 0.025 ^c
30 units	5.24 \pm 0.08	0.703 \pm 0.136 ^c	0.586 \pm 0.110 ^c	0.412 \pm 0.096 ^c	0.326 \pm 0.070 ^c	0.195 \pm 0.032
Osmolality <i>mOsm/kg</i>						
Vehicle	0.00	963.8 \pm 128.3	991.1 \pm 61.2	1012.6 \pm 74.2	1081.7 \pm 54.4	1093.8 \pm 72.7
1 unit	0.18 \pm 0.01	1254.3 \pm 100.8	1243.3 \pm 71.1	103.3 \pm 87.9	1099.1 \pm 95.6	1074.0 \pm 31.1
3 units	0.54 \pm 0.01	853.9 \pm 115.4	1083.2 \pm 83.3	996.6 \pm 75.3	955.8 \pm 68.6	1258.5 \pm 178.3
10 units	1.72 \pm 0.03	1200.2 \pm 119.2	997.8 \pm 62.9	1023.1 \pm 110.8	1043.4 \pm 117.2	920.2 \pm 116.2
30 units	5.24 \pm 0.08	258.4 \pm 99.2	1156.4 \pm 62.5	931.8 \pm 73.7	1291.3 \pm 81.7	1019.1 \pm 101.6

Abbreviations are: $\text{U}_{\text{Na}}\text{V}$, sodium excretion; $\text{U}_{\text{K}}\text{V}$, potassium excretion.

^aTimed vehicle- and baseline- (preinjected) control values were determined as described in Table 1. Plasma and urinary sodium, potassium, osmolality, and creatinine were obtained prior to and after each time point (0, 20, 40, 60, 80, and 120 minutes) from the timed vehicle-control and peptide-treated groups. Baseline (preinjected) controls were: urinary flow, $1.89 \pm 0.16 \mu\text{L/min}$; glomerular filtration rate, $188.1 \pm 50.3 \mu\text{L/min}$; $\text{U}_{\text{Na}}\text{V}$, $0.694 \pm 0.099 \mu\text{Eq/min}$; $\text{U}_{\text{K}}\text{V}$, $0.223 \pm 0.043 \mu\text{Eq/min}$; osmolality, $950.1 \pm 60.3 \text{ mOsm/kg}$.

^bValues are means \pm standard error of the mean ($N = 6$ to 8 mice/group).

^c $P \leq 0.05$ compared to the respective timed-vehicle control group.

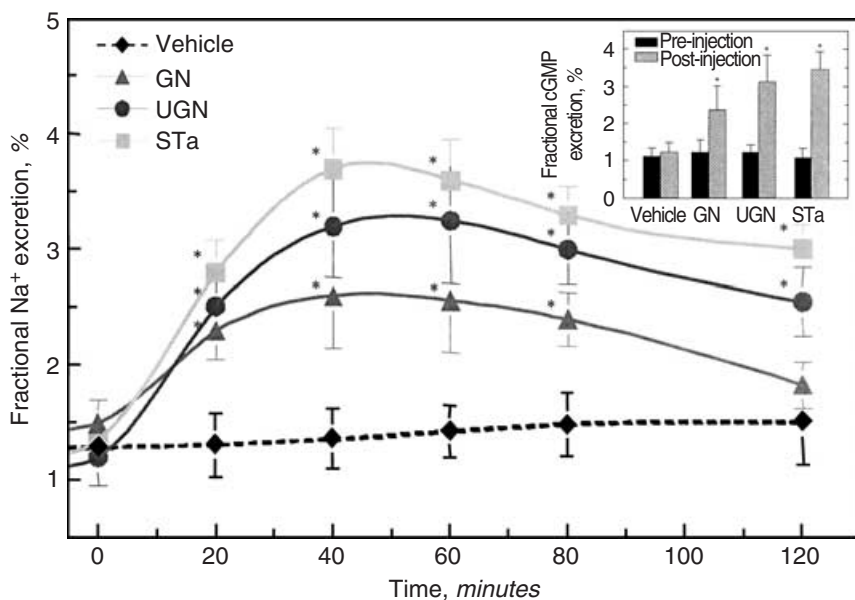


Fig. 1. Fractional sodium excretion and urinary cyclic guanosine monophosphate (cGMP) concentration following the intravenous administration of guanylin (GN), uroguanylin (UGN), and heat-stable enterotoxin (STa) in mice. Mice were treated with 10 units of peptide (GN, $64.4 \mu\text{g/kg}$; UGN, $18.8 \mu\text{g/kg}$; STa, $1.72 \mu\text{g/kg}$) or vehicle as described in Tables 1 to 3. Fractional Na^+ excretion (%) is shown as a function of time for GN, UGN, STa, and vehicle. Inset: Urinary cGMP levels (expressed as fractional cGMP excretion, FE_{cGMP}) were assessed at 60 minutes postpeptide injection. Values are means \pm standard error of the mean ($N = 6$ -8 mice/group per time point) and each point represents the total fractional excretion for that specific time point (i.e., six to eight mice were used to determine the FE_{Na} at 20 minutes, six to eight were used to determine the FE_{Na} at 40 minutes, and so on). * $P < 0.05$ compared to the respective timed-vehicle control group.

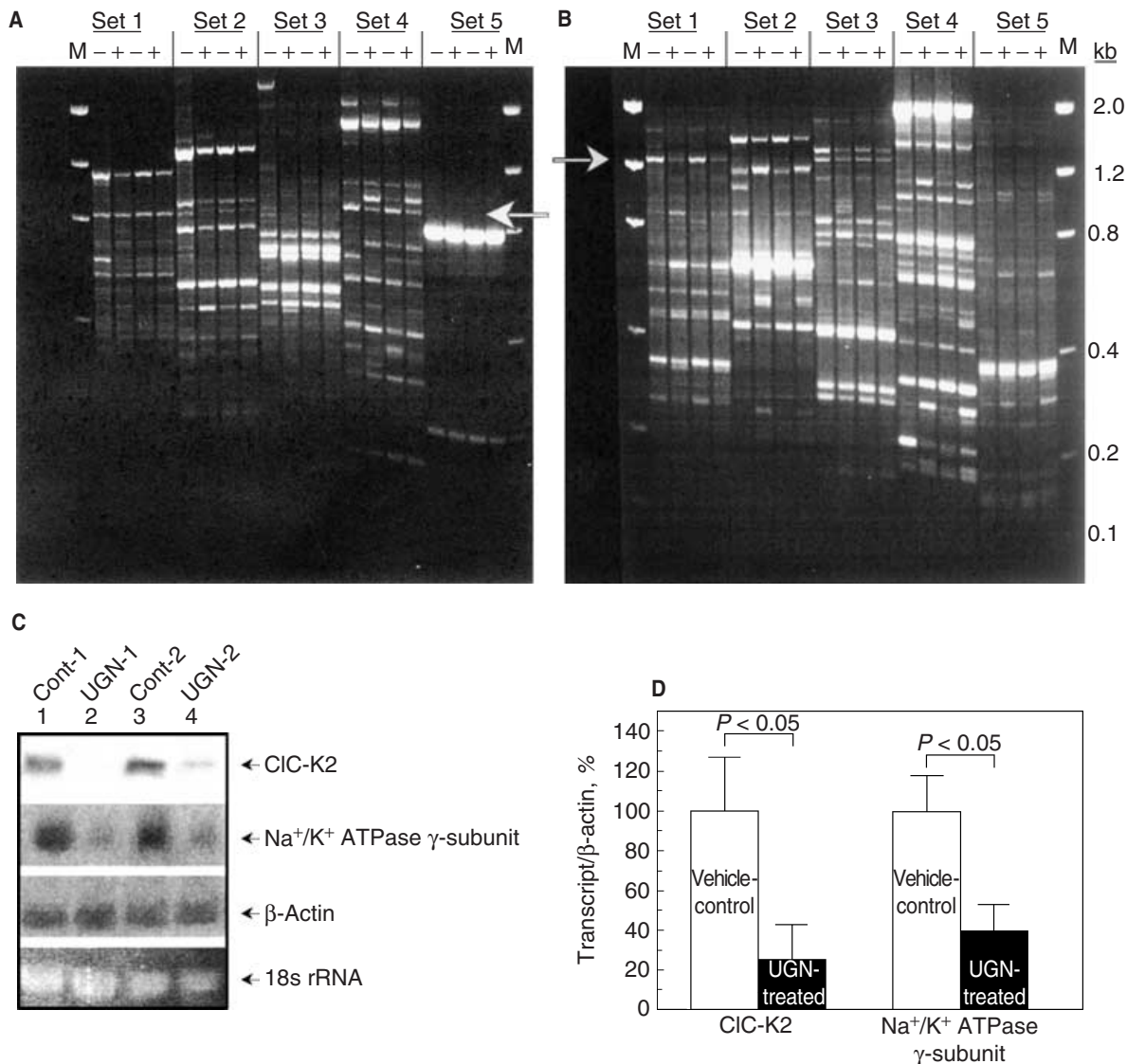


Fig. 2. Molecular changes in kidney by intravenous uroguanylin (UGN) treatment. Differential display-polymerase chain reaction (DD-PCR) and Northern analysis were performed using kidney RNA from mice treated (bolus 50 μ L injection via tail-vein) with vehicle or UGN (18.8 μ g/kg body weight). (A and B) The DD-PCR profile from 10 arbitrary primer sets using DNase-treated kidney RNA from four separate mice, two control vehicle-treated mice (–), and two UGN-treated mice (+). Arrows identify two specific amplified products (A, Set 4) and (B, Set 1) that were excised from the gel, reamplified, subcloned, and sequenced. M is the size markers in kilobases (kb). (C) Representative Northern blot of kidney RNA from mice treated with vehicle (Cont-1, Cont-2) or UGN (UGN-1, UGN-2). cDNA probes directed against the mouse CIC-K2 chloride channel protein, Na⁺/K⁺ ATPase γ -subunit, and β -actin were used during hybridization. Arrows indicate the transcripts for each product. The 18s rRNA staining represents equal loading of the samples. (D, Relative expression, as assessed by Northern analyses, of the CIC-K2 chloride channel mRNA and the Na⁺/K⁺ ATPase γ -subunit mRNA normalized to β -actin expression ($N = 3$).

To further evaluate the renal effects of UGN, we examined changes in the molecular expression pattern of the kidney induced by UGN after intravenous administration by differential display-PCR (DD-PCR) (Fig. 2). Control mice ($N = 2$) were treated with an intravenous injection of vehicle only, whereas the experimental mice ($N = 2$) were treated with bioactive UGN. UGN- and vehicle-treated mice responded in a similar fashion to that shown in Table 2. Multiple amplified products were both up- and down-regulated compared to the control group (Fig. 2).

The arrows in Figure 2A and B are two PCR-amplified products that were further investigated. Translation from the sequence of the ~ 1.0 kb cDNA amplification product (Fig. 2A) corresponded to the CIC-K2 chloride channel protein and, as previously shown [12], the sequence from the ~ 1.3 kb cDNA product (Fig. 2B) translated into the Na⁺/K⁺ ATPase γ -subunit. To confirm that both of these mRNA species were truly down-regulated in mouse kidney 60 minutes following intravenous UGN treatment, we performed Northern analysis on whole kidney

Table 4. Summary of uroguanylin (UGN)-regulated kidney differential display clones

Clone ^a	Estimated size ^b bp	Effect of UGN treatment ^c	Identity/homology ^d
A:2-0455	455	Up	Cyclic adenosine monophosphate (cAMP)-dependent protein kinase II- β -subunit
A:3-0405	405	Up	Transcription factor ATF-4
A:4-1020	1020	Up	Extracellular signal-related kinase (ERK-1)
A:4-1000	1000	Down	CIC-K2
B:1-1300	1300	Down	Na ⁺ /K ⁺ -ATPase γ -subunit
B:2-0990	990	Up	RhoB
B:3-1300	1300	Down	Hepatocyte nuclear factor (HNF) 4
B:5-0650	650	Up	Sodium hydrogen exchanger 1

^aClone is identified as panel #: primer set #: polymerase chain reaction (PCR) clone size.

^bSize of PCR clone is estimated by comparison to the migration of the molecular size standards in the polyacrylamide gel.

^cEffect of the PCR clone by UGN treatment was determined by DD-PCR signal comparison between vehicle and peptide treatment groups and confirmed by semiquantitative reverse transcription (RT)-PCR (by previously described methods [39]).

^dIdentity of each clone was determined by sequencing and comparison to GENEBank database.

Table 5. Comparison of guanylin (GN)-, uroguanylin (UGN)-, and heat-stable enterotoxin (STa)-induced changes in renal function in wild-type and GC-C knockout mice

Strain ^a	Urinary flow $\mu\text{L}/\text{min}$	$\text{U}_{\text{Na}}\text{V}$ $\mu\text{Eq}/\text{min}$	$\text{U}_{\text{K}}\text{V}$ $\mu\text{Eq}/\text{min}$	FE_{Na} %	FE_{K} %	Cyclic guanosine monophosphate/ creatinine nmol/mg	Osmolality mOsm/kg	Number
Wild-type mice								
Vehicle-control ^{b,c}	1.83 ± 0.36	0.39 ± 0.09	0.39 ± 0.10	1.88 ± 0.21	27.4 ± 4.3	11.1 ± 2.9	848.6 ± 78.3	7
Guanylin	$3.75 \pm 0.70^{\text{d}}$	$1.48 \pm 0.31^{\text{d}}$	$0.99 \pm 0.25^{\text{d}}$	$3.51 \pm 0.39^{\text{d}}$	$47.0 \pm 7.5^{\text{d}}$	$26.5 \pm 4.9^{\text{d}}$	816.3 ± 58.8	5
Uroguanylin	$3.88 \pm 0.42^{\text{d}}$	$1.64 \pm 0.40^{\text{d}}$	$0.95 \pm 0.30^{\text{d}}$	$3.74 \pm 0.44^{\text{d}}$	$43.7 \pm 8.0^{\text{d}}$	$26.9 \pm 6.9^{\text{d}}$	862.9 ± 86.5	5
STa	$4.00 \pm 0.55^{\text{d}}$	$1.88 \pm 0.38^{\text{d}}$	$1.11 \pm 0.33^{\text{d}}$	$4.17 \pm 0.55^{\text{d}}$	$46.1 \pm 9.2^{\text{d}}$	$28.5 \pm 6.3^{\text{d}}$	890.7 ± 110.6	5
GC-C ^(-/-) null mice								
Vehicle-control	2.25 ± 0.29	0.29 ± 0.07	0.35 ± 0.09	0.91 ± 0.10	23.2 ± 3.7	14.0 ± 3.4	924.8 ± 34.0	5
Guanylin	$3.38 \pm 0.60^{\text{d}}$	$1.07 \pm 0.25^{\text{d}}$	$1.08 \pm 0.22^{\text{d}}$	$2.81 \pm 0.41^{\text{d}}$	$58.3 \pm 8.6^{\text{d}}$	$30.9 \pm 6.8^{\text{d}}$	992.0 ± 77.2	5
Uroguanylin	$3.50 \pm 0.51^{\text{d}}$	$1.34 \pm 0.39^{\text{d}}$	$1.21 \pm 0.38^{\text{d}}$	$3.40 \pm 0.52^{\text{d}}$	$51.4 \pm 10.0^{\text{d}}$	$37.9 \pm 8.2^{\text{d}}$	900.2 ± 92.1	5
STa	$3.67 \pm 0.49^{\text{d}}$	$1.47 \pm 0.50^{\text{d}}$	$1.42 \pm 0.41^{\text{d}}$	$3.56 \pm 0.59^{\text{d}}$	$64.5 \pm 11.3^{\text{d}}$	$36.4 \pm 5.6^{\text{d}}$	1002.3 ± 109.2	5

Abbreviations are: $\text{U}_{\text{Na}}\text{V}$ = sodium excretion; $\text{U}_{\text{K}}\text{V}$ = potassium excretion; FE_{Na} = fractional excretion of sodium; FE_{K} = fractional excretion of potassium.

^aWild-type mice are S129/Sv-Black Swiss hybrids; Homozygous GC-C^(-/-) null mice were obtained by intercrossing heterozygotes and are thus hybrids of 129/Sv-Black Swiss

^bTimed (60 minute) vehicle-control values were determined as described previously in Table 1. Vehicle or peptide (dissolved in vehicle) was administered by tail-vein injection (50 μL bolus). The urine was collected and measured 60 minutes postinjection. Plasma and urinary sodium, potassium, osmolality, and creatinine were obtained after each 60-minute time point from the timed vehicle-control and peptide-treated groups.

^cValues are means \pm standard error of the mean ($N = 5-7$ mice/group).

^d $P \leq 0.05$ compared to the respective timed-vehicle control group.

RNA from mice treated with UGN or vehicle. Shown in Figure 2C and D, both the CIC-K2 and the Na⁺/K⁺ ATPase γ -subunit transcripts are decreased upon UGN treatment by over 75% and 60%, respectively. Additional cDNA products were removed from the differential display gels, purified, and subjected to semiquantitative RT-PCR, as previously reported [12, 32]. A list of products (confirmed by PCR product sequence analysis) and their approximate size is shown in Table 4. Further characterization of these potentially important cDNAs and their impact on UGN signaling and regulation in the kidney are currently being investigated through quantitative RT-PCR and Northern analyses.

Renal effects of GN, UGN, and STa in GC-C^(-/-) null mice

To determine whether the effects of GN and UGN in the kidney are mediated by its cognate receptor,

GC-C, we employed the in vivo modified renal function assay in mice deficient of GC-C (GC-C^(-/-) null) [41]. These knockout mice were originally developed to test for the impact of GC-C-mediated physiologic events in the intestine. However, since recent studies have shown the agonists for this receptor exhibit renal properties, we hypothesized the renal effects of GN, UGN, and STa would be attenuated in GC-C^(-/-) null mice. Using an optimum time and concentration of the peptides in the assay (as determined in Tables 1 to 3), GC-C^(-/-) null mice responded to exogenous GN, UGN, and STa in a similar fashion to normal wild-type mice (Table 5). In fact, in both wild-type and GC-C^(-/-) null mice, GN, UGN, and STa all independently increased urine volume and urinary sodium concentrations by over twofold and fourfold, respectively. In addition, fractional sodium excretion in GC-C^(-/-) null mice was significantly increased by GN (3.1-fold), UGN (3.7-fold), and STa (3.9-fold) when compared to vehicle

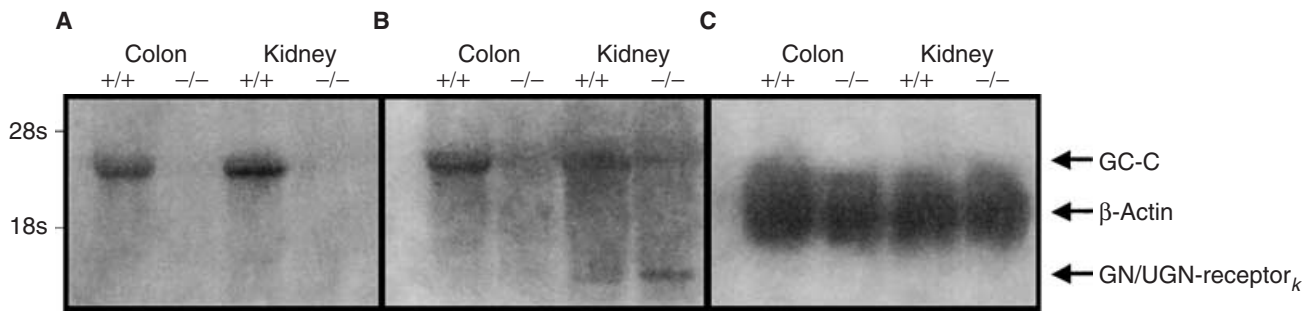


Fig. 3. Northern blot analysis of wild-type and GC-C^(-/-) null mouse RNA from colon and kidney cortex. (A) Hybridization of RNA from wild-type (+/+) and GC-C^(-/-) null (-/-) mouse colon and kidney cortex with a mouse GC-C cDNA probe (Assn ID #BC034064, IMAGE clone 4208530) reveals the absence of the 3.8 kb GC-C transcript from the GC-C^(-/-) null mouse. (B) Hybridization using the renal 400 bp polymerase chain reaction (PCR) product from the GC-C^(-/-) null mouse kidney indicates the presence of a 3.8 kb transcript containing a guanylin (GN)/uroguanylin (UGN) binding site region in wild-type mouse colon and kidney cortex (probably GC-C), and a 2.5 kb transcript in wild-type and GC-C^(-/-) null mouse kidney cortex (GN/UGN-receptor_k). (C) β -actin hybridization to the same blot.

control-treated mice, which were similar to the peptide-induced responses observed in wild-type mice. Furthermore, elevations in urinary cGMP were associated with increased sodium excretion. In wild-type mice, the peptides increased the urinary levels of cGMP by approximately 2.5-fold. In GC-C^(-/-) null mice, urinary cGMP was increased over the control-group by 2.2-fold (GN), 2.7-fold (UGN), and 2.6-fold (STa). Potassium excretion was also significantly increased by 2.5- to 2.7-fold in wild-type and GC-C^(-/-) null mice by all three peptides. The osmolalities in the wild-type or knockout mice did not significantly differ between the vehicle- or peptide-treated groups. Thus, in mice, the effect of GN, UGN, and STa are mediated, in part, by a GC-C independent mechanism.

Northern analysis of wild-type and GC-C^(-/-) null mouse RNA

Using colon and renal cortex RNA from wild-type and GC-C^(-/-) null mice, Northern analysis was performed using two different molecular probes directed against the GN/UGN receptor: (1) the intracellular catalytic domain of wild-type mouse GC-C (Assn ID #BC034064), and (2) a 400 bp PCR product homologous to the GC-C ligand-binding homology domain from the GC-C^(-/-) null mouse kidney. The signal at approximately 3.8 kb demonstrates the presence of GC-C in the colon of wild-type mice (Fig. 3A). Also, as previously shown, this 3.8 kb GC-C transcript is absent in colonic RNA isolated from GC-C^(-/-) null mice [41]. Similarly, the message for GC-C is absent in kidney RNA from GC-C^(-/-) null mice. When using the same blot probed with the 400 bp PCR GC-C-like product from GC-C^(-/-) null mice, a signal at 3.8 kb in the wild-type colon and kidney is observed (Fig. 3B). However, an alternative, smaller signal of ~2.5 kb is also observed in the wild-type and GC-C^(-/-) null mouse kidney. This smaller transcript is absent in RNA isolated from colonic tissue.

DISCUSSION

Considerable evidence exists suggesting that GN and UGN play an important role in salt and water regulation in the kidney [12, 14, 32–34, 37, 39, 49–51]. This report describes that exogenous GN, UGN, and their bacterial mimic peptide STa, administered intravenously, not only increase sodium and potassium excretion in vivo, but that the renal effects are time- and dose-dependent. The most significant increase in sodium and potassium excretion was observed approximately 40 minutes following intravenous administration of each peptide. In addition, the time-dependent increase in fractional sodium excretion by these peptides was associated with a significant increase in urinary cGMP and a decrease in GFR, suggesting that GN, UGN, and STa elicit their effects in a renal tubular, rather than a hemodynamic, mechanism.

Current data are consistent with the concept that GN and UGN can affect renal function by binding to GC-C receptors located on several nephron segments [32, 34, 37, 52–54]. However, data from this report suggests that GN and UGN are able to elicit natriuretic and kaliuretic effects in a GC-C-independent mechanism (Table 5). One possible explanation for these results is that alternative GN/UGN/STa receptors exist in the kidney. In wild-type mice, the physiologic effects of these peptides may be due to a combination of both GC-C and the alternative receptor(s). This concept is supported by our preliminary molecular studies demonstrating the presence of two distinct mRNA transcripts (3.8 and 2.3 kb) using GC-C-like molecular probes (Fig. 3). In addition, GC-C-independent cellular and physiologic responses to GN, UGN, and STa have been described in the kidney [37, 50]. For example, a UGN-induced mechanism was found to regulate ion conductances (and mediate electrogenic electrolyte transport) specifically within isolated collecting duct cells from GC-C^(-/-) null mice [50]. The precedence of an alternate receptor for natriuretic

peptides, however, is not unusual. Atrial natriuretic peptide binds to a guanylate cyclase-coupled receptor, guanylate cyclase-A (GC-A), and a truncated clearance receptor (NPC-R) that is devoid of the intracellular protein kinase-like and guanylate cyclase domains [55]. NPC-R functions to decrease the bioavailability of secreted natriuretic peptides (ANP, BNP, CNP) in neural, renal, and vascular tissue and/or modulate cAMP-driven second messenger cascades [56]. In fact, agonist binding to NPC-R in endothelial cells inhibits cAMP production via a G_i protein-coupled signaling system. Thus, an alternate receptor for GN and/or UGN may exist in the kidney that also regulates renal sodium and chloride transport.

Based on the existing literature, at least two potential confounds should be taken into consideration. First, it has yet to be established where functional GC-C or alternate GN/UGN receptors are located within specific nephron segments. Our previous data would suggest that primary sites of action would include the proximal convoluted tubule, medullary thick ascending limb, and the cortical collecting tubules as targets for GN, UGN, and STa [32]. Thus, further detailed segmental analysis employing *in vivo* micropuncture and *in vitro* micropertusion are necessary to identify specific nephron segments containing functional GN/UGN/STa sites of action. Second, it is quite possible that GN, UGN, and STa may act by modulating the effects of other ligands on renal tubular transport. For example, studies with ANP showed that it has no effect on basal proximal tubule fluid reabsorption, but attenuates angiotensin II stimulated transport [57]. In this regard, Santos et al [58] have made the somewhat paradoxical observation that UGN can attenuate the ANP-induced increase in fractional sodium and potassium excretion in the isolated perfused rat kidney.

Under normal physiologic conditions, GN and UGN circulate in the bloodstream [34, 53, 54, 59–64]. The primary source of these peptides has been proposed to be the intestine [9, 63, 65]. Two separate groups have recently found that these peptides are secreted basolaterally as well as from the apical/luminal surface of intestinal cells [18, 63]. The expression and/or secretion of intestinal GN and UGN is affected *in vivo* by acute salt intake, and *in vitro*, by hypertonic solutions [18, 37, 39, 53, 59, 66]. In fact, our laboratory has recently shown that rats on a low salt diet have lower circulating levels of GN and UGN than rats on a normal- or high-salt diet [abstract; Greenberg RN et al, *FASEB J* 17:A1074, 2003]. In contrast, plasma concentrations of UGN by Fukae et al [49], in rats on a low- and high-salt diet did not significantly differ, although the urinary excretion of UGN was significantly higher in rats on the high-salt diet compared to those on a low-salt diet. Furthermore, UGN mRNA expression in the kidney, as well as urinary sodium and cGMP excretion, significantly correlated with the increased urinary UGN levels.

The response to salt intake and the natriuretic activity of these intestinal peptides has led to the hypothesis that GN and UGN may participate in an enterorenal control system. In this system, changes in dietary NaCl intake lead to the appropriate changes in intestinal and plasma levels of GN and UGN, which in turn, alter renal sodium excretion. The idea of an intestinal natriuretic factor(s) is supported by the fact that the natriuretic response of the kidney to an increased sodium load occurs faster when the load is delivered orally than when the same load is delivered intravenously [7–9]. There are well-established precedents for such feed-forward control systems within the gastrointestinal tract. For example, glucose-dependent insulinotropic peptide is released from the intestine in response to ingestion of a meal and, in turn, stimulates the pancreatic release of insulin prior to increases in plasma glucose concentration [67]. The intent of this report was to rigorously evaluate the renal effects of GN and UGN in a modified mouse clearance model that lends itself to addressing questions concerning the physiologic role of these peptides and their postulated endocrine role in sodium regulation. Our studies suggest a renal role for GN and UGN. Significant responses (i.e., increased sodium and potassium excretion) induced by these peptides are observed within 20 minutes and are continued until the end point of the assay (120 minutes). It is interesting to note that UGN induces a greater fractional sodium excretion than GN, which may be due to the inherent differences in primary and secondary structure of these peptides [9, 14, 24].

We compared the activity of GN, UGN, and STa following a 2-hour incubation of the peptides in mouse plasma. These stability studies were performed prior to injecting the peptides into mice. GN, UGN, and STa appear to be stable in plasma, with ~95% or more of the peptide activity being retained after incubation (data not shown). The results for STa are similar to that observed in humans [68]. These data suggest that all three peptides should retain appropriate biologic activity in the modified mouse clearance studies, and thus, bind to and activate renal GN/UGN/STa receptors.

Associated with the natriuretic response induced by UGN in mice were changes in the mRNA levels of a series of kidney-specific transport-associated proteins. One of the putative gene products isolated by DD-PCR coded for the γ -subunit of the Na^+/K^+ ATPase, which constitutes one of the major sodium pumps in the kidney. Our results suggest that intravenous UGN treatment induces a down-regulation of the Na^+/K^+ ATPase γ -subunit mRNA and quite possibly, the protein. The γ -subunit itself is a small, type I membrane protein localized on the basolateral membranes of epithelial cells and is expressed in the medullary thick ascending limb, distal convoluted tubules, and the inner medullary collecting duct [46]. It specifically modulates the activity of

the Na^+/K^+ ATPase, which maintains the membrane potential, the Na^+ -gradient, and the transepithelial voltage difference that energize transcellular, Na^+ -coupled and paracellular ion transport [69]. The function and regulation of the γ -subunit is quite complex. However, reports have suggested that it is a nephron/tissue-specific regulator of the Na^+/K^+ ATPase, modulating the affinity of sodium, potassium, and ATP [69, 70]. Thus, down-regulation of γ -subunit mRNA could, in turn, decrease the driving force for the reabsorption of sodium in specific nephron segments in a long-term fashion.

Exogenous UGN administration also affected the kidney-specific chloride channel ClC-K2 . This particular chloride channel plays an important role in the transepithelial reabsorption of chloride ions and is most abundantly expressed along the basolateral surface of the medullary thick ascending limb, cortical collecting tubules, and the distal tubules [71, 72]. The physiologic significance of ClC-K2 in the kidney has not yet been completely elucidated. However, previous reports suggest that it serves as a route for transcellular chloride transport (i.e., an exit for chloride ions in the basolateral plasma membrane of ClC-K2 -containing nephron segments)[73]. In fact, loss-of-function mutations of ClC-K2 lead to a loss of chloride ions from the body and have been implicated in Bartter's syndrome [71]. Down-regulation of this channel protein (e.g., by UGN) may, in turn, lead to the decrease of chloride reabsorption and increase urinary levels of sodium and chloride.

Clearly, it should be noted that gene expression data does not necessarily indicate changes in protein expression. Also, UGN may cause the changes in Na^+/K^+ ATPase γ -subunit and ClC-K2 , but this observation does not establish cause and effect. To define the role of these proteins in GN/UGN-induced natriuresis, studies are planned with the current model using natriuretic peptides other than GN, UGN, and STa in wild-type and $\text{GC-C}^{(-/-)}$ null mice. If the transcripts that encode Na^+/K^+ ATPase γ -subunit and ClC-K2 do not change upon intravenous administration of nonguanylin peptides, one would assume that GN, UGN, and STa play a direct role in the decrease of the molecular expression of these peptides, and hence, potentially influence long-term renal function. The same experiment performed in $\text{GC-C}^{(-/-)}$ null mice could also be used to determine the role of and control for the alternate UGN receptor on Na^+/K^+ ATPase and ClC-K2 . If these genes are not down-regulated in $\text{GC-C}^{(-/-)}$ null mice upon UGN treatment, then the argument that Na^+/K^+ ATPase γ -subunit and/or ClC-K2 are unrelated to changes in electrolyte excretion is stronger. However, as shown in Tables 1 to 3 and Figure 1, natriuresis occurs in a rapid and transient fashion (less than 90 minutes). Physiologic changes (i.e., natriuresis) due to modifications in gene and protein expression have not been reported within the timeframe observed

for GN and UGN action (40 minutes). Thus, the decrease in molecular expression Na^+/K^+ ATPase γ -subunit or ClC-K2 mRNA may not contribute to the rapid-onset and transient natriuresis induced by GN and UGN. A secondary natriuretic response in mice may occur hours after the initial exposure of the nephron to GN and UGN. Further experiments are currently being performed to examine the long-term effects of GN and UGN in the wild-type and $\text{GC-C}^{(-/-)}$ null mouse kidney.

Sodium excretion by the kidney needs to be precisely regulated. Even small increases in sodium intake in the absence of compensatory changes in the rate of tubular sodium reabsorption would rapidly lead to life-threatening salt retention [74, 75]. Daily fluctuations in sodium intake would necessitate, at most, a change of only a few percent in tubular reabsorption [1, 2, 74]. GN and UGN may provide the body with such a mechanism, whereby ingested salt regulates the expression and secretion of these peptides from intestinal cells into the circulation, and in turn, affects tubular sodium reabsorption via GN/UGN receptors lining the nephron. We describe in this report that even low levels of these intestinal natriuretic peptides affect renal sodium excretion in a transient, but time-dependent fashion. Further studies are obviously necessary to clarify and quantify the effect of alterations in and mechanisms of NaCl intake on GN/UGN synthesis and secretion, and the resultant changes in renal transport. Molecular studies characterizing the novel GN/UGN receptor are also warranted and are currently underway in our laboratory. However, taken together, our studies suggest that GN and UGN may act on the mouse kidney causing significant natriuresis by an alternate GN/UGN/STa receptor, GC-C -independent mechanism via renal tubular processes. Long-term renal effects by UGN may also affect sodium transport by inhibiting the activity and/or down-regulating the expression of specific sodium and chloride channels, such as Na^+/K^+ ATPase and ClC-K2 .

ACKNOWLEDGMENTS

The authors would like to dedicate this report to the memory of Congmei Sun; we were blessed with the time she spent with us and we will miss her.

This work was supported by the Office of Research and Development, Medical Research Service, Department of Veterans Affairs, Lexington, Kentucky (R.N.G., B.A.J., and S.L.C.), Cincinnati, Ohio (R.A.G. and L.E.M.), and Columbia, Missouri (L.R.F.); the American Cancer Society (S.L.C.); and the National (B.A.J.) and Ohio Affiliate of the American Heart Association (C.E.O.).

Reprint requests to Stephen L. Carrithers, Ph.D., University of Kentucky, Division of Infectious Diseases, VA Medical Center, Research Service 151-CDD, 1101 VA Drive, VAMC D-309, Lexington, KY 40506.
E-mail: SLCARU0@uky.edu

REFERENCES

1. WEINBERGER MH: *Hypertension: Pathophysiology, Diagnosis, and Management*. New York, Raven, 1990

2. GARBERS DL, DUBOIS SK: The molecular basis of hypertension. *Annu Rev Biochem* 68:127–155, 1999
3. CAREY RM, SMITH JR, ORT EM: Gastrointestinal control of sodium excretion in sodium-depleted rabbits. *Am J Physiol* 230:1504–1508, 1976
4. CAREY RM: Evidence for a splanchnic sodium input monitor regulating renal sodium excretion in man: Lack of dependence upon aldosterone. *Circulation Res* 43:19–23, 1978
5. LUNDGREN O, HANSSON GC: Is there an intestinal natriuretic factor? *Acta Physiol Scandinavica* 141:19–25, 1991
6. MU JY, HANSSON GC, LUNDGREN O: The intestinal tract and the pathophysiology of arterial hypertension: An experimental study on Dahl rats. *Acta Physiol Scandinavica* 155:137–146, 1995
7. MU JY, HANSSON GC, LUNDGREN O: Renal sodium excretion after oral or intravenous sodium loading in sodium-depleted normotensive and spontaneously hypertensive rats. *Acta Physiol Scandinavica* 153:169–177, 1995
8. MU JY, HANSSON GC, LUNDGREN O: The small intestine, salt intake and arterial hypertension. *Blood Pressure* 4:77–79, 1995
9. FORTE LR, FAN X, HAMRA FK: Salt and water homeostasis: Uroguanylin is a circulating peptide hormone with natriuretic activity. *Am J Kidney Dis* 28:296–304, 1996
10. LENNANE RJ, CAREY RM, GOODWIN TJ, PEART WS: A comparison of natriuresis after oral and intravenous sodium loading in sodium-depleted man: Evidence for a gastrointestinal or portal monitor of sodium intake. *Clin Sci Mol Med* 49:437–440, 1975
11. LENNANE RJ, PEART WS, CAREY RM, SHAW J: A comparison of natriuresis after oral and intravenous sodium loading in sodium-depleted rabbits: Evidence for a gastrointestinal or portal monitor of sodium intake. *Clin Sci Mol Med* 49:433–437, 1975
12. CARRITHERS SL, HILL MJ, JOHNSON BR, et al: Renal effects of uroguanylin and guanylin in vivo. *Braz J Med Biol Res* 32:1337–1344, 1999
13. FORTE LR, LONDON RM, FREEMAN RH, KRAUSE WJ: Guanylin peptides: Renal actions mediated by cyclic GMP. *Am J Physiol* 278:F180–F191, 2000
14. FONTELES MC, GREENBERG RN, MONTEIRO HS, et al: Natriuretic and kaliuretic activities of guanylin and uroguanylin in the isolated perfused rat kidney. *Am J Physiol* 275:F191–F197, 1998
15. FORTE LR, LONDON RM, KRAUSE WJ, FREEMAN RH: Mechanisms of guanylin action via cyclic GMP in the kidney. *Annu Rev Physiol* 62:673–695, 2000
16. GARBERS DL: Guanylyl cyclase receptors and their ligands. *Adv Second Messenger Phosphoprotein Res* 28:91–95, 1993
17. VAANDRAGER AB: Structure and function of the heat-stable enterotoxin receptor/guanylyl cyclase C. *Mol Cell Biochem* 230:73–83, 2002
18. STEINBRECHER KA, RUDOLPH JA, LUO G, COHEN MB: Coordinate upregulation of guanylin and uroguanylin expression by hypertonicity in HT29-18-N2 cells. *Am J Physiol* 283:C1729–C1737, 2002
19. MARTIN S, ADERMAN K, FORSSMANN WG, KUHN M: Regulated, side-directed secretion of proguanylin from isolated rat colonic mucosa. *Endocrinology* 140:5022–5029, 1999
20. KUHN M, ADERMAN K, JAHNE J, et al: Segmental differences in the effects of guanylin and *Escherichia coli* heat-stable enterotoxin on Cl^- secretion in human gut. *J Physiol* 479:433–440, 1994
21. STEINBRECHER KA, MANN EA, GIANNELLA RA, COHEN MB: Increases in guanylin and uroguanylin in a mouse model of osmotic diarrhea are guanylate cyclase C-independent. *Gastroenterology* 121:1191–1202, 2001
22. FIELD M, GRAF LH, LAIRD WJ, SMITH PL: Heat-stable enterotoxin of *E. coli*: In vitro effects of guanylate cyclase activity, cyclic GMP concentration, and ion transport in small intestine. *Proc Natl Acad Sci USA* 75:2800–2804, 1978
23. CARPICK BW, GARIEPY J: The *Escherichia coli* heat-stable enterotoxin is a long-lived superagonist of guanylin. *Infect Immun* 61:4710–4715, 1993
24. GREENBERG RN, HILL M, CRYTZER J, et al: Comparison of effects of uroguanylin, guanylin, and *Escherichia coli* heat-stable enterotoxin STa in mouse intestine and kidney: Evidence that uroguanylin is an intestinal natriuretic hormone. *J Inv Med* 45:276–283, 1997
25. SANTOS-NETO MS, CARRITHERS SL, MONTEIRO HSA, et al: Guanylin and its lysine-containing analogue in the isolated perfused rat kidney: Interaction with chymotrypsin inhibitor. *Pharm Toxicol* 92:114–120, 2003
26. FORTE LR, KRAUSE WJ, FREEMAN RH: Guanylin bioactivity in human intestinal and opossum kidney cells. *Adv Second Messenger Phosphoprotein Res* 28:133–138, 1993
27. FORTE LR, KRAUSE WJ, FREEMAN RH: *Escherichia coli* enterotoxin receptors: Localization in opossum kidney, intestine, and testis. *Am J Physiol* 257:F874–F881, 1989
28. FORTE LR, KRAUSE WJ, FREEMAN RH: Receptors and cGMP signaling mechanisms for *E. coli* enterotoxin in opossum kidney. *Am J Physiol* 255:F1040–F1046, 1988
29. KRAUSE WJ, LONDON RM, FREEMAN RH, FORTE LR: The guanylin and uroguanylin peptide hormones and their receptors. *Acta Anat (Basel)* 160:213–231, 1997
30. FURUYA S, NARUSE S, ANDO E, et al: Effect and distribution of intravenously injected ^{125}I -guanylin in rat kidney examined by high-resolution light microscopic radioautography. *Anat Embryol (Berl)* 196:185–193, 1997
31. KRAUSE WJ, FREEMAN RH, FORTE LR: Autoradiographic demonstration of specific binding sites for *E. coli* enterotoxin in various epithelia of the North American opossum. *Cellular Tissue Res* 260:387–394, 1990
32. CARRITHERS SL, TAYLOR B, CAI WY, et al: Guanylyl cyclase-C receptor mRNA distribution along the rat nephron. *Regulatory Pep* 95:65–74, 2000
33. LONDON RM, EBER SL, VISWESWARIAH SS, et al: Structure and activity of OK-GC: A kidney receptor guanylate cyclase activated by guanylin peptides. *Am J Physiol* 276:F882–F891, 1999
34. KINOSHITA H, FUJIMOTO S, NAKAZATO M, et al: Urine and plasma levels of uroguanylin and its molecular forms in renal diseases. *Kidney Int* 52:1028–1034, 1997
35. KITA T, KITAMURA K, SAKATA J, ETO T: Marked increase of guanylin secretion in response to salt loading in the rat small intestine. *Am J Physiol* 277:G960–G966, 1999
36. MORO F, LEVENEZ F, NEMOZ-GAILLARD E, et al: Release of guanylin immunoreactivity from the isolated vascularly perfused rat colon. *Endocrinology* 141:2594–2599, 2000
37. POTTHAST R, EHLER E, SCHEVING LA, et al: High salt intake increases uroguanylin expression in mouse kidney. *Endocrinology* 142:3087–3097, 2001
38. LI Z, KNOWLES JW, GOYEAU D, et al: Low salt intake down-regulates the guanylin signaling pathway in rat distal colon. *Gastroenterology* 111:1714–1721, 1996
39. CARRITHERS SL, JACKSON BA, CAI WY, et al: Site-specific effects of dietary salt intake on guanylin and uroguanylin mRNA expression in rat intestine. *Regulatory Pep* 107:87–95, 2002
40. SCHULZ S, GREEN CK, YUEN PS, GARBERS DL: Guanylyl cyclase C is a heat-stable enterotoxin receptor. *Cell* 63:941–948, 1990
41. MANN EA, JUMP ML, WU J, et al: Mice lacking the guanylyl cyclase C receptor are resistant to STa-induced intestinal secretion. *Biochem Biophys Res Commun* 239:463–466, 1997
42. GIANNELLA RA: Suckling mouse model for detection of heat-stable *Escherichia coli* enterotoxin: characteristics of the model. *Inf Immun* 12:95–99, 1976
43. CARRITHERS SL, EBER SL, FORTE LR, GREENBERG RN: Increased urinary excretion of uroguanylin in patients with congestive heart failure. *Am J Physiol* 278:H538–H547, 2000
44. HAMRA FK, EBER SL, CHIN DT, et al: Regulation of intestinal uroguanylin and guanylin receptor-mediated responses by mucosal acidity. *Proc Natl Acad Sci USA* 94:2705–2710, 1997
45. CURRIE MG, FOK KF, KATO J, et al: Guanylin: an endogenous activator of intestinal guanylate cyclase. *Proc Natl Acad Sci USA* 89:947–951, 1992
46. MERCER RW, BEIMESDERFER D, BLISS DP, Jr, et al: Molecular cloning and immunological characterization of the γ -polypeptide, a small protein associated with the Na^+ , K^+ -ATPase. *J Cell Biol* 121:579–586, 1993
47. TAKEUCHI Y, UCHIDA S, MARUMO F, SAKAKI S: Cloning, tissue distribution, and intrarenal localization of CIC chloride channels in human kidney. *Kidney Int* 48:1497–1503, 1995
48. FONTELES MC, MONTEIRO HS, SOARES AM, et al: The lysine-1 analog of guanylin induces intestinal secretion and natriuresis in the isolated perfused kidney. *Braz J Med Biol Res* 29:267–271, 1996

49. FUKAE H, KINOSHITA H, FUJIMOTO S, *et al*: Changes in urinary levels and renal expression of uroguanylin on low or high salt diets in rats. *Nephron* 92:373–378, 2002
50. SINDICE A, BASOGLU C, CERCI A, *et al*: Guanylin, uroguanylin, and heat-stable enterotoxin activate guanylate cyclase C and/or a pertussis toxin-sensitive G protein in human proximal tubule cells. *J Biol Chem* 277:17758–17764, 2002
51. FAN X, WANG Y, LONDON RM, *et al*: Signaling pathways for guanylin and uroguanylin in the digestive, renal, central nervous, reproductive, and lymphoid systems. *Endocrinology* 138:4636–4648, 1997
52. KINOSHITA H, FUJIMOTO S, YOKOTA N, *et al*: Uroguanylin acts as a natriuretic factor via guanylate cyclase C. *J Am Soc Nephrol* 8:A1863–A1863, 1997
53. KINOSHITA H, FUJIMOTO S, FUKAE H, *et al*: Plasma and urine levels of uroguanylin, a new natriuretic peptide, in nephrotic syndrome. *Nephron* 81:160–164, 1999
54. NAKAZATO M, YAMAGUCHI H, KINOSHITA H, *et al*: Identification of biologically active and inactive human uroguanylin in plasma and urine and their increases in renal insufficiency. *Biochem Biophys Res Commun* 220:586–593, 1996
55. HEMPLE A, NOLL T, BACH C, *et al*: Atrial natriuretic peptide clearance receptor participates in modulating endothelial permeability. *Am J Physiol* 275:H1818–H1825, 1998
56. HERMAN JP, DOLGAS CM, MARCINEK R, LANGUB MCJ: Expression and glucocorticoid regulation of natriuretic peptide clearance receptor (NPR-C) mRNA in rat brain and choroid plexus. *J Chem Neuroanat* 11:257–265, 1996
57. EITLE E, HIRANYACHATTADA S, WANG H, HARRIS PJ: Inhibition of proximal tubular fluid absorption by nitric oxide and atrial natriuretic peptide in rat kidney. *Am J Physiol* 274:C1075–C1080, 1998
58. SANTOS NETO MS, CARVALHO AF, FORTE LR, FONTELES MC: Relationship between the actions of atrial natriuretic peptide (ANP), guanylin and uroguanylin on the isolated kidney. *Braz J Med Biol Res* 32:1015–1019, 1999
59. KINOSHITA H, NAKAZATO M, YAMAGUCHI H, *et al*: Increased plasma guanylin levels in patients with impaired renal function. *Clin Nephrol* 47:28–32, 1997
60. FUKAE H, KINOSHITA H, FUJIMOTO S, *et al*: Plasma concentration of uroguanylin in patients on maintenance dialysis therapy. *Nephron* 84:206–210, 2000
61. KUHN M, RAIDA M, ADERMAN K, *et al*: The circulating bioactive form of human guanylin is a high molecular weight peptide (10.3 kDa). *FEBS Lett* 318:205–209, 1993
62. NAKAZATO M, YAMAGUCHI H, SHIOMI K, *et al*: Identification of 10-kDa proguanylin as a major guanylin molecule in human intestine and plasma and its increase in renal insufficiency. *Biochem Biophys Res Commun* 205:1966–1975, 1994
63. KUHN M, KULAKSIZ H, CETIN Y, *et al*: Circulating and tissue guanylin immunoreactivity in intestinal secretory diarrhoea. *Eur J Clin Invest* 25:899–905, 1995
64. DATE Y, NAKAZATO M, YAMAGUCHI H, *et al*: Tissue distribution and plasma concentration of human guanylin. *Intern Med* 35:171–175, 1996
65. LI ZP, PERKINS AG, PETERS MF, *et al*: Purification, cDNA sequence, and tissue distribution of rat uroguanylin. *Regulatory Pep* 68:45–56, 1997
66. STEINBRECHER KA, MANN EA, GIANNELLA RA, COHEN MB: A hypertonic diet increases mouse guanylin and uroguanylin levels via a guanylate cyclase C-independent mechanism. *Gastroenterology* 120:3671, 2001
67. BROWN JC, OTTE SC: GIP and the entero-insular axis. *Clin Endocrinol Metab* 8:365–377, 1981
68. GALI H, SIECKMAN GL, HOFFMAN TJ, *et al*: Chemical synthesis of *Escherichia coli* ST(h) analogues by regioselective disulfide bond formation: biological evaluation of an (111)In-DOTA-Phe(19)-ST(h) analogue for specific targeting of human colon cancers. *Bioconjug Chem* 13:224–231, 2002
69. MEI IC, KOENDERINK JB, VAN BOKHOVEN H, *et al*: Dominant isolated renal magnesium loss is caused by misrouting of the Na⁺,K⁺-ATPase γ -subunit. *Nature Genetics* 26:265–266, 2000
70. ARYSTARKHOVA E, DONNET C, ASINOVSKI NK, SWEADNER KJ: Differential regulation of renal Na⁺, K⁺-ATPase by splice variants of the γ -subunit. *J Biol Chem* 277:10162–10172, 2002
71. UCHIDA S: In vivo role of CLC chloride channels in the kidney. *Am J Physiol* 279:F802–F808, 2000
72. YOSHIKAWA M, UCHIDA S, YAMAUCHI A, *et al*: Localization of rat CLC-K2 chloride channel mRNA in the kidney. *Am J Physiol* 45:F552–F558, 1999
73. WOLF K, CASTROP H, RIEGGER GAJ, *et al*: Differential gene regulation of renal salt entry pathways by salt load in the distal nephron of the rat. *Pflügers Archives-Eur J Physiol* 442:498–504, 2001
74. JACKSON BA, OTT CE: *Renal System*, Madison, CT, Fence Creek Publishing LLC, 1999
75. DiBONA GF, KOPP UC: Neural control of renal function. *Physiol Rev* 77:75–197, 1997